Thermal Desorption of Carbon Monoxide from Model Interstellar Ice Surfaces: Revealing Surface Heterogeneity

Monthly Notices
of the
ROYAL ASTRONOMICAL SOCIETY

MNRAS **498,** 1693–1699 (2020)
Advance Access publication 2020 September 3

doi:10.1093/mnras/staa2372

Thermal desorption of carbon monoxide from model interstellar ice surfaces: revealing surface heterogeneity

S. Taj and M. R. S. McCoustra ★

Institute of Chemical Sciences, Heriot-Watt University, Edinburgh, EH14 4AS, UK

Accepted 2020 August 4. Received 2020 August 4; in original form 2020 July 13

ABSTRACT

Temperature programmed desorption has been used to probe the distribution of binding energies of carbon monoxide (CO) to molecular solid thin films of astrophysical relevance. Measurements are reported for solid water (both compact amorphous solid water and crystalline water), ammonia, and methanol surfaces. Binding energy distributions and optimized pre-exponential factors based on the inversion method are tabulated. These are compared to existing data on these systems and astrophysical conclusions drawn.

Key words: astrochemistry – solid state: volatile – methods: laboratory: solid state.

1 INTRODUCTION

Since the 1990s, temperature programmed desorption (TPD) has become the *de facto* method for experimentally determining adsorbate binding energies, E_b, in laboratory astrophysics (Minissale et al., in preparation). As most systems of astrophysical interest express physisorption behaviour, where interactions are determined by simple electrostatics and dispersion, that is, van der Waals interactions and hydrogen bonding rather than electron exchange, E_b and the *activation energy for desorption*, $E_{\rm des}$, are equal in magnitude but opposite in sign (equation 1):

$$E_b = -E_{\rm des} \tag{1}$$

Thus, non-equilibrium (kinetic or dynamical) measurements of the rate of desorption, $r_{\rm des}$, given by the Polanyi–Wigner equation (Attard & Barnes 1998):

$$r_{\rm des} = \frac{{\rm d}n_{\rm ads}}{{\rm d}t} = \nu_{\rm des}\ (n_{\rm ads})\,(n_{\rm ads})^m {\rm e}^{-E_{\rm des}(n_{\rm ads})/RT} \tag{2}$$

where m is the order of desorption, $n_{\rm i,\ ads}$ is the surface concentration, and $\nu_{\rm des}$ is the surface concentration-dependent pre-exponential factor; are alone sufficient to determine $E_{\rm des}$ and its surface concentration dependence. A dependence on surface concentration reflects both the presence of multiple binding sites of varying binding energy on the surface, and the presence of adsorbate–adsorbate interactions.

TPD is a long established technique in surface science (Woodruff & Delchar 1994) which has been revolutionized in recent years by the adoption of line-of-sight methods developed by Jones (Hessey & Jones 2015). Simply, under conditions of high pumping speed, changes in partial pressure measured by quadrupole mass spectrometer (QMS) can be shown to be proportional to $r_{\rm des}$. Analysis of TPD data is well described in the literature and given the order of desorption can be approached through a hierarchy of approaches (King 1975). These stretch from the simplest assumption of a surface concentration independent $E_{\rm des}$ obtained from simple Arrhenius-like analysis at a fixed coverage; through inversion analysis yielding monolayer $E_{\rm des}$ distributions assuming a fixed pre-exponential factor based on Redhead (1962) and Hasegawa, Herbst & Leung (1992) of 10^{12} s^{-1}; to the recent work of Kay and coworkers (Tait et al. 2005a, b, c; Smith, May & Kay 2016) where an optimized pre-exponential factor and monolayer $E_{\rm des}$ distribution are obtained.

Solid CO is the second most abundant species found in astrophysical ices after water ice. Equilibrium measurements of CO adsorption on porous amorphous solid water (ASW) have been reported by Allouche, Verlaque & Pourcin (1998). Values for the isosteric enthalpy of adsorption ranging from −9.7 to −10.3 kJ mol^{-1} are reported for a number of ASW samples at temperatures between 43 and 48 K. This is a hint towards heterogeneity of the solid H_2O surface and a distribution of CO binding energies on that surface.

A detailed surface science study of the CO-H_2O system followed (Collings et al. 2003a, b). While the focus of this work was clearly on the role of trapping of CO in the ice, a kinetic analysis of the TPD data yielded desorption parameters for CO solid [$E_{\rm des} = 6{:}9 \pm 0{:}2$ kJ mol^{-1} and $\nu_{\rm des} = (7 \pm 2) \times 10^{26}$ cm^{-2} s^{-1}] and for the monolayer of CO adsorbed on solid H_2O [$E_{\rm des} = 9.8 \pm 0{:}2$ kJ mol^{-1} and $\nu_{\rm des} = (5 \pm 1) \times 10^{14}$ s^{-1}]. The single activation energy for desorption of CO from the solid H_2O surface ensures adequate reproduction of the experimental data. However, tailing of the TPD data to high temperatures suggests that this might be a woefully inadequate description of the interaction of CO with a porous amorphous solid H_2O surface. Indeed, in the paper, this tailing is discussed in terms of CO diffusion into the porous structure of the substrate over the solid H_2O surface and out of the porous structure *via* gaseous diffusion. However, the commonality of the trailing edges and the lowering of the peak desorption temperature for CO leaving the solid H_2O surface with increasing coverage is entirely consistent with first-order desorption from a heterogeneous surface exposing a range of binding sites and hence a distribution of binding energies. Kay and coworkers have recently measured this distribution (Smith, May & Kay 2016) and report binding energies ranging from 11 to nearly 17 kJ mol^{-1} with an optimized pre-exponential factor of

★ E-mail: M.R.S.McCoustra@hw.ac.uk

3.5×10^{16} s^{-1}. Even in the simpler case of compact ASW, where trapping and diffusion are limited, three independent studies (Noble et al. 2012; Fayolle et al. 2016; He, Acharyya & Vidali 2016) have used fixed pre-exponential factors derived from the harmonic approximation of Hasegawa, Herbst & Leung (1992) of 7.1×10^{11} s^{-1}, or from the work of Redhead (1962) of 1.0×10^{12} s^{-1}, and obtained binding energy distributions ranging from 8.3 to 12.4 kJ mol^{-1}. None of which we can now see is representative in the light of the more recent and detailed work of Smith, May & Kay (2016).

This paper reports on TPD investigations of carbon monoxide (CO) adsorbed on molecular solid surfaces relevant to astrophysical environments. Data will be presented on the binding energy distributions and optimized pre-exponential factor derived using the method of Smith, May & Kay (2016) for CO desorbing from solid water (crystalline and compact amorphous), solid ammonia (amorphous), and solid methanol (amorphous).

2 EXPERIMENTAL

The experiments were performed in an ultrahigh vacuum (UHV) apparatus described in detail elsewhere (Fraser, Collings & McCoustra 2002). The apparatus comprises a cylindrical stainless steel chamber pumped, to an operating pressure of 2×10^{-10} mbar, by a combination of liquid-nitrogen trapped oil diffusion pump and mechanical rotary pump (Edwards E06 and E2M18, respectively). The substrate, an oxygen-free high conductivity copper block evaporatively coated with 200–300 nm of amorphous silica ($aSiO_2$) (Thrower et al. 2009) is mounted on the end of a closed-cycle helium-cooled cryostat mounted in an UHV XYZθ sample manipulator. Surface temperatures on the substrate in the range 15–500 K are monitored by a KP-type (Au-Chromel) thermocouple. A line-of-sight QMS (Hiden Analytical Ltd, HAL301) was employed in the TPD measurements reported in this paper.

CO was deposited by background dosing onto thick (100s of molecular layers) films of solid water, methanol, and ammonia that themselves were grown by background dosing on the $aSiO_2$-coated substrate. Crystalline water (CSW) films were grown with substrate at 140 K and compact ASW (c-ASW) with the substrate at 100 K. While amorphous films of both methanol and ammonia were grown on an 18 K substrate. Typically, exposures of several hundred Langmuir (L; 1 L $\equiv 1 \times 10^{-6}$ mbar s) were employed to ensure that there was complete coverage of the underlying $aSiO_2$.

The substrate ice films were exposed to CO doses in the range 1–25 L (1–15 L for the ammonia film) covering the transition from sub-monolayer to multilayer film in order to allow identification of the monolayer dose and permit the CO coverage to be expressed in terms of fractions or multiples of a monolayer. TPD is performed by applying a heating ramp of 0.1–0.5 K s^{-1} to a suitable final surface temperature.

3 RESULTS AND DISCUSSION

Taj (2019) summarizes the experimental details and describes the methodology employed in correcting the raw TPD data for an exponentially increasing background signal. Fig. 1 presents an illustrative subset of this TPD data. The transition from sub-monolayer desorption to multilayer desorption can be readily identified from the changes in the TPD profile from common trailing edges and maximum temperatures moving to lower values with increasing exposure consistent with first order sub-monolayer and monolayer desorption from a distribution of binding sites to common leading edges consistent with zero-order multilayer desorption. We can

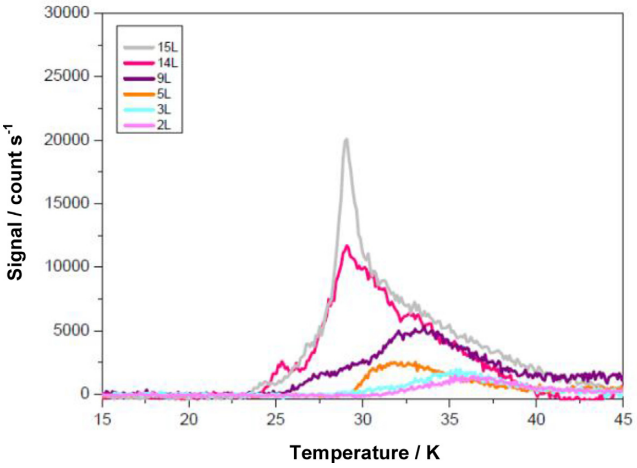

Figure 1. Experimental TPD data for desorption of CO from a CSW surface. Exposures are reported in Langmuir.

identify that 1 ML is equivalent to an exposure of 9 L on each of our solid substrates. This allows us to place the TPD data on a coverage scale from 0 to 1 ML (ML = monolayer) and to correctly identify the data for inversion analysis.

Since the assumption of a single value for E_{des} is no longer valid, we must apply direct inversion of the Polanyi–Wigner equation (2). This gives E_{des} as function of the surface concentration at time t, $N(t)$:

$$E_{des} = -RT \ln\left(\frac{dn_{ads}/dt}{\nu_{des} n_{ads}(t)^m}\right) \quad (3)$$

This technique was first reported by Tait et al. (2005a, b, c) and has since been adapted to describe small molecule desorption from similarly heterogeneous astrophysically-relevant surfaces (see e.g. Thrower et al. 2009a, b; Noble et al. 2012; Collings et al. 2015; Fayolle et al. 2016; He, Acharyya & Vidali 2016). To determine $n_{ads}(t)$, the initial surface concentration ($n_{ads,\,tot}$) is assumed to be given by the rate of bombardment (Z_W) multiplied by the dose time (τ) (equation 4):

$$n_{ads,tot} = Z_w \tau = \frac{PS\tau}{\sqrt{2\pi m k_B T}} \quad (4)$$

where P is the pressure, S is the sticking coefficient, and m is the mass of a CO molecule. At the low surface temperatures used in this study, the flux of species leaving the surface either directly upon collision or desorbing is believed to be relatively small, making S near unity. The values of $n_{ads}(t)$ are obtained by subtracting the total gas phase concentration at the previous time-step from the initial surface concentration ($n_{ads,\,tot}$). The values of dn_{ads}/dt are determined by the experimental TPD data. Within the sub-monolayer regime, m is assumed to be 1. We then depart from the previous formulation of the inversion procedure and employ the method of Smith, May & Kay (2016). For a fixed, but variable, value of ν in the range $10^{12\pm10}$ s^{-1}, plots of E_{des} against $n_{ads}(t)$ are constructed for each CO sub-monolayer dose on each substrate and averaged to give the full range of E_{des} *versus* n_{ads} on each substrate.

Fig. 2 illustrates this for CO desorption from CSW. The corresponding data for the other substrates are given in Taj (2019). The data shown in Fig. 2 are in line with those reported by Noble et al. (2012), which range between 11.1 and 8.4 kJ mol^{-1} as the coverage increases toward the full monolayer. Similar figures are presented

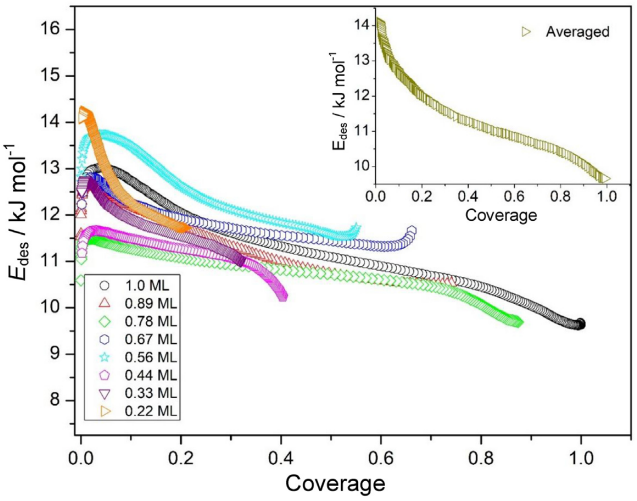

Figure 2. $E_{\rm des}$ *versus* coverage for sub-monlayer quantities of CO desorbing from CSW deposited at 140 K. The inset shows the averaged data. The plots were obtain using the optimized pre-exponential factor, $\nu_{\rm des}$, of $2.51^{+1.47}_{-0.93} \times 10^{17}$ s^{-1}.

in the electronic Supporting Information to this paper for the other systems studied.

A functional fit is then made to the averaged $E_{\rm des}$ *versus* coverage data to obtain the $E_{\rm des}(n_{\rm ads})$ function. Kinetic simulations using this function are then based on a FORTRAN 90 program developed in the work of Thrower (2009) and revised by Taj (2019). The experimental time and surface temperatures are taken as input and the program coding altered for each $E_{\rm des}$ coverage dependence function to calculate the desorption rate through the Polanyi–Wigner equation (2). The output data contain the calculated desorption rate and value of $E_{\rm des}$ at each simulated time point.

Some typical simulations are displayed in Fig. 3 in comparison with the corresponding experimental data. The agreement is good; confirming that desorption of sub-monolayer quantities of CO from these substrates follows first-order kinetics with a range of desorption energies.

The pre-exponential factor, $\nu_{\rm des}$, is optimized by minimizing the sum of the squares of the residuals (5) over the potential range of $\nu_{\rm des}$ from 1×10^2 to 1×10^{22} s^{-1};

$$R^2 = \sum_{\rm coverage} \sum_t \left(n_{\rm ads,\ experimental}\,(t) - n_{\rm ads,simulated}\,(t)\right)^2 \qquad (5)$$

Fig. 4 shows R^2 for the comparison of the experimental and simulated TPD data for sub-monolayer coverage of CO desorbing from CSW *versus* the logarithm of the pre-exponential factor used in the inversion analysis. The solid line is a fit to the points and this gives, at the minimum of R^2, a value of $\nu_{\rm des}$ of $2.51^{+1.47}_{-0.93} \times 10^{17}$ s^{-1}.

Table 1 summarizes the optimized kinetic data for CO desorption from the substrate solids under study in comparison to known existing values from the literature. The corresponding $E_{\rm des}$ *versus* coverage plots derived in this work are shown in the electronic Supplementary Information as Figs ESI-1 (c-ASW), ESI-2 (solid methanol), and ESI-3 (solid ammonia).

There appears to be significant variation in the listed values which must reflect the nature of the surfaces and their interactions with CO. In particular, the pre-exponential values cover many orders of magnitude when in principle comparing the same system; as for example in the case of CSW and c-ASW. However, it can be seen that as the pre-exponential factor increases, this appears to be compensated for by an increase in the activation energy for desorption. This highlights the key issue that we must recognize in relation to TPD interpretation that we are measuring rates of desorption and the two parameters that we are using to describe the TPD process are linked *via* the Polyani–Wigner equation (2). For two interpretations of a sub-monolayer TPD data set yielding respectively, $E_{\rm des,1}(n_{\rm ads})$ and $\nu_{\rm des,1}(n_{\rm ads})$, and $E_{\rm des,2}(n_{\rm ads})$ and $\nu_{\rm des,2}(n_{\rm ads})$, it is obvious that since both were derived from the same rate data using equation (2) then equation (6) must hold true

$$r_{\rm des} = \nu_{\rm des,1}\,(n_{\rm ads})\,{\rm e}^{-E_{\rm des,1}(n_{\rm ads})/T} = \nu_{\rm des,2}\,(n_{\rm ads})\,{\rm e}^{-E_{\rm des,2}(n_{\rm ads})/T} \qquad (6)$$

and either interpretation is therefore equally valid in describing the desorption kinetics.

Table 1 also allows us to make two additional points. The first relates to the assumption that desorption from a complex substrate can be described by a single activation energy for desorption. This is simply not true as both the experimental and computational literatures are demonstrated. Both heterogeneity in the adsorbate–substrate interaction, reflecting the variety of binding sites on the surface, and adsorbate–adsorbate interactions, reflecting the coverage dependence of the adsorption process, play a role in determining the activation energy for desorption.

The second point naturally arises if we accept the first. To invert experimental TPD data to a distribution of activation energies for desorption, an assumption must be made about the pre-exponential factor. Within the Transition State Theory framework, $\nu_{\rm des}$ is given by the ratio of the partition function of the adsorbate in the physisorption well, and its partition function in the transition state on the pathway to desorption:

$$\nu_{\rm des} = \frac{k_B}{h}\,\frac{Q^{\ddagger}}{Q_{\rm ads}} \qquad (7)$$

where $Q_{\rm ads}$ is the partition function for the adsorbed state, $Q^{\ddagger}$ is the partition function for the transition state, k_B is the Boltzmann constant, and h is the Planck constant. In the limit of desorption of a physisorbed atom, $Q^{\ddagger}/Q$ is approximately unity and consequently $\nu_{\rm des}$ lies in the range is 10^{12}–10^{13} s^{-1}. Both Redhead (1962) and Hasegawa, Herbst & Leung (1992) adopt this assumption. With molecular adsorbates, the additional internal degrees of freedom in the molecule must be considered as must the conversion of the restricted rotations and translations of the molecule on the surface into free rotations and translations in the transition state. Taking such contributions to $Q_{\rm ads}$ and $Q^{\ddagger}$ into account, this ratio, and hence, $\nu_{\rm des}$ can reach significantly larger values. For example, in the adsorption of functionalized alkanes, alcohols and ethers on graphite, $\nu_{\rm des}$ values are found to be around 10^{19} s^{-1} (Doronin et al. 2015).

From the thermodynamic formulation of Transition State Theory, $\nu_{\rm des}$ is found to be related to the activation entropy for desorption, $\Delta^{\ddagger}S$:

$$\nu_{\rm des} = \frac{k_B T}{h} \exp\left(\frac{\Delta^{\ddagger} s}{R}\right) \qquad (8)$$

where R is the gas constant. $\Delta^{\ddagger}S$ represents the entropy difference in taking the adsorbate from its initial state, $S_{\rm ads}$, to the transition state, $S^{\ddagger}$:

$$\Delta^{\ddagger} S = S^{\ddagger} - S_{\rm ads} \qquad (9)$$

Hence, estimating the entropy of activation allows the pre-exponential factor to be calculated. There are two limiting situations. In the case of a *tight transition state*, the entropy of the transition state itself is reduced compared to that of the adsorbed molecule. While in a *loose transition state* situation, the transition state has extra degrees of freedom and hence higher entropy than the adsorbed

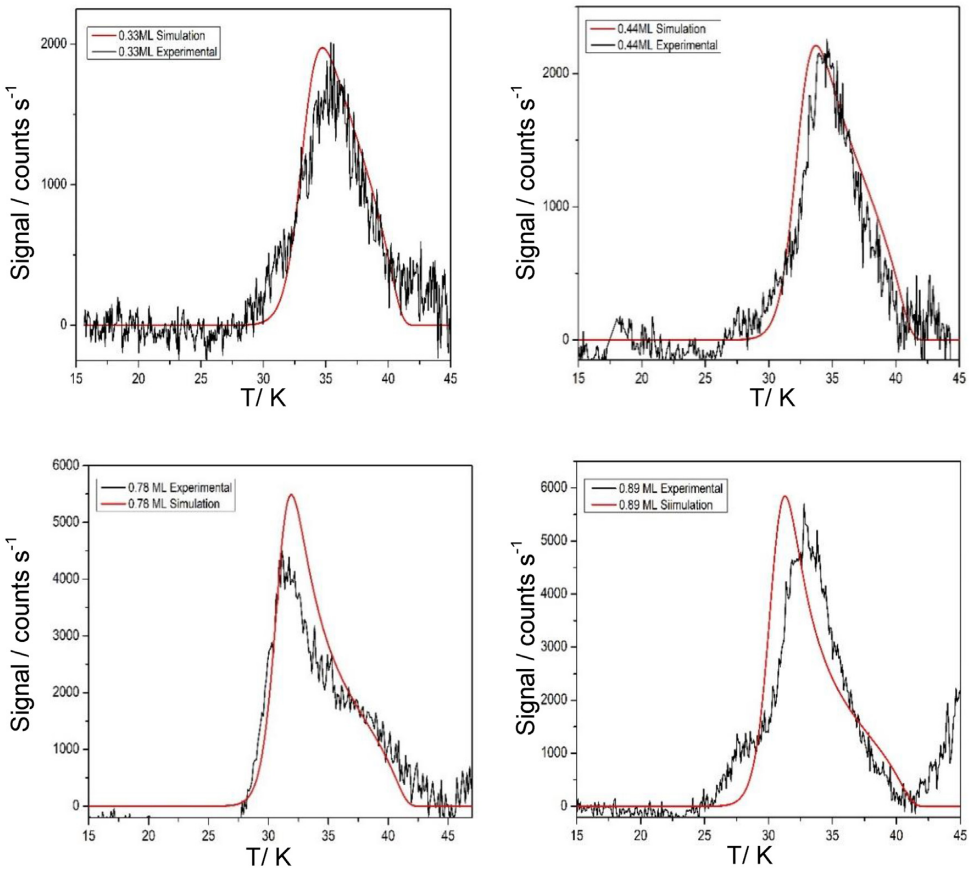

Figure 3. A comparison of the experimental (red) and simulated (black) TPD spectra for sub-monolayer quantities of CO on CSW. The simulated spectra were obtained using the $E_{\rm des}(\theta)$ curve in Fig. 2 obtained using a pre-exponential factor of $2.51^{+1.47}_{-0.93} \times 10^{17}$ s^{-1}. The variability in the comparison of the measured and simulated TPD is a consequence of the global fitting procedure used to derive the optimal $\nu_{\rm des}$ and corresponding variation of $E_{\rm des}$ with coverage.

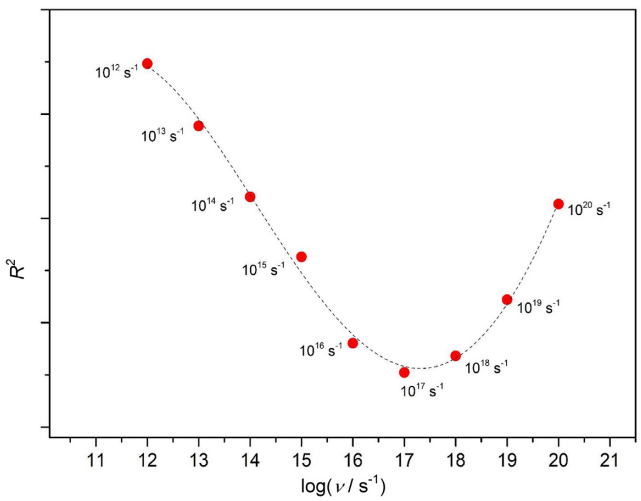

Figure 4. The R^2 between the experimental and simulated TPD for CO desorbing from CSW for all quantities of CO initially on the CSW surface *versus* the pre-exponential factor used in the Extended Inversion Analysis. The fitted broken line yields a minimum at 17.40 ± 0.20 corresponding to a best-fitting value of $\nu_{\rm des}$ of $2.51^{+1.47}_{-0.93} \times 10^{17}$ s^{-1}.

molecule. Consequently, ν is typically greater than 10^{13} s^{-1} with a loose transition state and less than 10^{13} s^{-1} with a tight transition state. Recognizing that S^{+} can be written in term of the gas phase entropy of the adsorbed molecule, $S_{\rm gas}$, less the entropy associated with the 1D translation that is motion along the desorption coordinate, $S_{\rm gas,1D\text{-}trans}$, an estimate of the actual pre-exponential factor can be made using:

$$\nu = \frac{k_B T}{h} \exp\left(\frac{S_{\rm gas} - S_{\rm gas,1D-trans} - S_{\rm ads})}{R}\right) \quad (10)$$

Campbell et al. (2012) have been able to extend this by demonstrating that for many systems $S_{\rm ads}$ linearly tracks the entropy of the gas-phase molecule at the same temperature, such that

$$\frac{S_{\rm ads}}{R} = 0.70\frac{S_{\rm gas}}{R} - 3.30 \quad (11)$$

with a standard deviation of only $2R$ over a range of $50R$. Adding the appropriate Sackur–Tetrode term for the 1D translation lost to the desorption coordinate, Campbell et al. were then make reliable estimates of the pre-exponential factor in physisorption systems with attractive adsorbate–adsorbate interactions using equation (12):

$$\nu_{\rm des} = \frac{k_b T}{h} \exp\left\{\frac{0.30 S_{\rm gas}}{\rm R} + 3.3 - (1/3) \times \left\{18.6 + \ln\left[(m/m_{\rm Ar})^{3/2}(T/298\,{\rm K})^{5/2}\right]\right\}\right\} \quad (12)$$

where m is the molar mass of the gas and $m_{\rm Ar}$ is the molar mass of Argon. T is the measurement temperature corresponding to the peak desorption rate. Table 2 presents estimates of $\Delta^{+}S$ for

Table 1. Compilation and comparison of kinetic parameters for CO desorption from relevant astrophysical solids.

	ν_{des} (s^{-1})	E_{des} (kJ mol^{-1})	Reference
H_2O surfaces			
p-ASW (15 K)	5.00×10^{14}	9.8	Collings et al. (2003a, b)
ASW (60 K)	9.80×10^{14}	11.8–17.0	Smith et al. (2015)
c-ASW (100 K)	1.00×10^{11}	13.1–9.6	Fayolle et al. (2016)
Non-porous ASW (100 K)	1.00×10^{12}	10.7–7.2	Penteado et al. (2017)
c-ASW (100 K)	$2.57^{+1.04}_{-1.21} \times 10^{15}$	12.5–9.5	This work
CSW (140 K)	1.00×10^{12}	11.1–8.4	Noble et al. (2012)
CSW (140 K)	$2.51^{+1.47}_{-0.93} \times 10^{17}$	14.2–9.5	This work
CH_3OH surfaces			
Amorphous CH_3OH (15 K)	$1.41^{+0.29}_{-0.45} \times 10^{16}$	14.0–12.8	This work
NH_3 surfaces			
Amorphous NH_3 (15 K)	$1.51^{+0.46}_{-0.40} \times 10^{12}$	8.5–8.4	This work

Table 2. Entropies of activation derived from the listed pre-exponential factors, cf. the value calculated by the method of Campbell et al. (2012) of 86.8 J K^{-1} mol^{-1}.

Surface	ν (s^{-1})	$\Delta^{\ddagger}S$ (J K^{-1} mol^{-1})
c-ASW	$2.57^{+1.04}_{-1.21} \times 10^{15}$	$67.91^{+1.28}_{-1.11}$
CSW	$2.51^{+1.47}_{-0.93} \times 10^{17}$	$106.00^{+1.28}_{-1.11}$
CH_3OH	$1.41^{+0.29}_{-0.45} \times 10^{16}$	$81.83^{+1.21}_{-1.05}$
NH_3	$1.51^{+0.46}_{-0.40} \times 10^{12}$	$5.59^{+1.21}_{-1.06}$

each of the systems studied derived by re-arranging equation (6). Application of equation (12) yields a value of 86.8 J K^{-1} mol^{-1}. This compares favourably with the experimentally derived values in Table 2 for c-ASW, CSW, and CH_3OH. These systems are clearly representative of loose transition states and reflecting the large heterogeneity expressed by the surface and represented in the measured broad range of activation energies for desorption in each of these systems.

The data in Table 2 on CO desorption from NH_3 contrast markedly with those of CO desorbing from the c-ASW, CSW, and CH_3OH surfaces. This clearly suggests that we are perhaps closer to the tight transition state limit in this case. Does it really make sense that the nature of the transition state would change in this one instance? No, such as change is unlikely. So what is significantly different? From Table 1, it is clear that the activation energy for desorption of CO from NH_3 is both smaller than those reported for the other substrates and expresses much less heterogeneity (i.e. a narrower spread of values). Indeed, if we accept the commonly reported correlation that the barrier to diffusion of a species on a surface is roughly 10–15 per cent of the activation energy for desorption (Nørskov et al. 2014), then CO is much more mobile on NH_3 than on the other substrates. This mobility must therefore increase the entropy of the adsorbed state, which consequently reduces the entropy of activation.

4 ASTROPHYSICAL IMPLICATIONS AND CONCLUSIONS

This work reinforces the observation that heterogeneity on the surfaces of thin films of molecular solids can yield a variation of binding energy with adsorbate coverage for a simple molecular probe like CO. The obvious question that arises astrophysically is then what value of binding energy to use in simulating thermal desorption of CO from these surfaces?

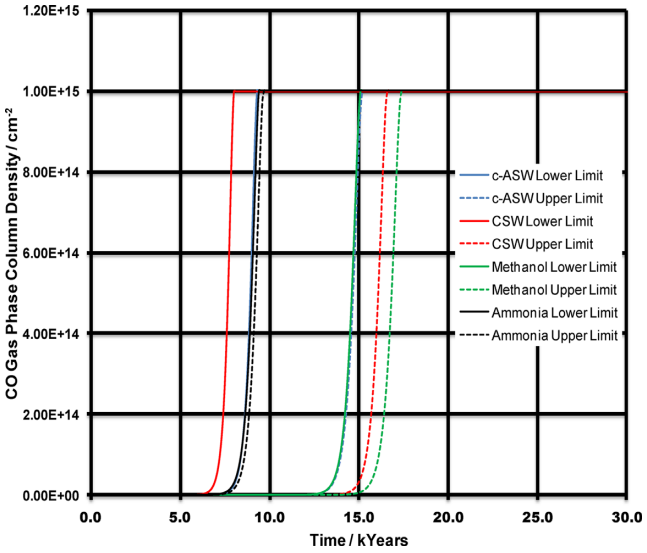

Figure 5. Simulations of thermal desorption of a CO monolayer from the model interstellar ice surfaces employed in this work. The heating rate in the model is assumed to be 1 K per millennium. The activation energies for desorption are taken as single valued from our E_{des} data in Table 2. The upper and lower limits refer to the maximum and minimum values of the range of E_{des} recovered by inversion and reported in Table 2.

Fig. 5 illustrates the variation in the temporal profile of 1 ML of CO (assumed in this instance to be 10^{15} molecules cm^{-2}) desorbing from the model ice surfaces explored in this work. The simulations integrate the Polyani–Wigner equation (2) for a single value of the activation energy for desorption, the optimized pre-exponential factor (Table 2) using simple Euler integration and assuming a heating rate of 1 K per millennium. Simulations are presented assuming the minimum and maximum E_{des} recovered from inversion of the experimental TPD data for each model interstellar ice and listed in Table 2.

As can be clearly seen from Fig. 5, where there is significant width in the range of E_{des} presented for CO desorbing from the model ice surface, then there can be significant delay in the desorption in comparing the minimum E_{des} to the maximum. Considering the example of CSW, where E_{des} ranges from 9.5 to 14.2 kJ mol^{-1}, we see that this can introduce as much as some 7500 yr delay in CO desorption. This disparity will increase with lower heating rates and decrease at higher rates. However, the key issue remains that

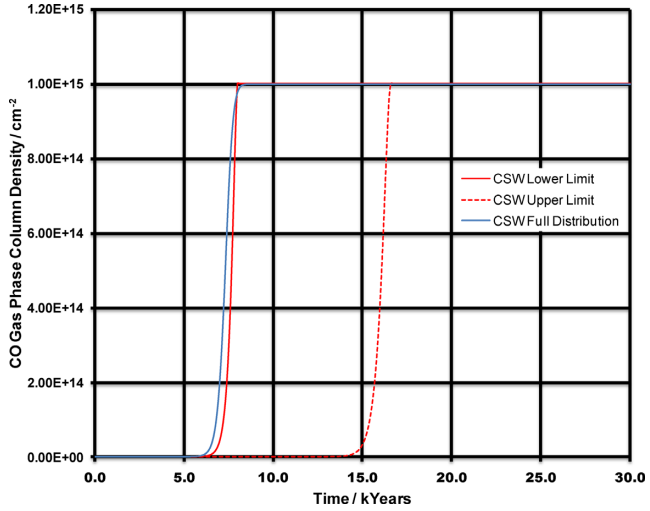

Figure 6. Simulations of thermal desorption of a CO monolayer from a CSW surface illustrating the impact of a coverage-dependent E_{des} as reported in Table 2 compared to the single-valued simulations reported in Fig. 5. The heating rate in the model is assumed to by 1 K per millennium.

assuming a single value of E_{des} does not reproduce the experimental data and therefore would be inappropriate in simulations of thermal desorption up to monolayer coverage. This could impact on any post-desorption gas-phase chemistry (Penteado et al. 2017).

Ideally, we should account for the coverage dependence of E_{des}. Fig. 6 illustrates such a simulation where the Polyani–Wigner equation (2) has been integrated using a functional description of the variation in E_{des} with coverage represented in the inset figure in Fig. 2; and assuming the optimized pre-exponential factor (Table 2) and a heating rate of 1 K per millennium. The temporal profile derived assuming the full distribution of E_{des} overlaps closely with the simulation for the minimum value of E_{des} in this instance. So in this instance, the minimum E_{des} might be a good representation of the E_{des} to use in modelling CO desorption from the CSW surface. However, it is clear that the desorption extends over a longer time-scale, approximately three times as long at around 3300 yr, when the full distribution of E_{des} in considered within the simulation presented in Fig. 6.

There are two additional points that should also be considered. In many simulations of multilayer desorption, first order kinetics are assumed, that is, layer-by-layer desorption of the multilayer films. These simulations are also subject to the limitations imposed by assuming a single E_{des}. The molecules comprising an ice may at the surface of that ice present a range of activation energies. For example, in ASW the H_2O molecules at the surface may be attached to the surface with a range of hydrogen bonding interactions. Consequently, it should never be assumed that in a layer-by-layer desorption that a single value of E_{des} may operate. Though, it is clear that the range of uncertainty on measured E_{des} values for multilayer films may hide what is likely to be a relatively narrow range of activation energies for desorption.

The second point is simply that the same distribution of E_{des} will equally apply in adsorption. Then when there is adsorption under conditions where molecules are free to explore the surface of the ice, CO will adsorb first at the most strongly bound sites; filling the surface with increasing weakly bound CO according to the coverage dependence in Fig. 2. However, in the situation where truly ballistic deposition is considered, the dependence in Fig. 2 will be explored randomly. Evidence from the IR spectroscopy of CO adsorbed at 15 K suggests the former situation holds true for CO deposition on typical dust and ice surfaces (Taj et al. 2017, 2019).

To conclude, in this paper we have reported detailed inversion analyses for CO desorbing from models of interstellar ices. We have reported the optimized pre-exponential factors and the range of binding energies expressed by each of the substrate ices that we have investigated. These have been used to illustrate the limitations of single E_{des} value simulations of thermal desorption. Of course, these experiments report on but one aspect of CO desorption from ices, that of the release of CO from the vacuum accessible surface of a pure ice. Investigation of such desorption from ice mixtures representative of those likely to be found in space would allow us to reflect on the impact of the surface composition of the ice on the variation of E_{des} with coverage on such systems. While bringing us closer to the complex reality that exists in space, such measurements might allow us to demonstrate whether or not a simple proportionally additive approach based on data derived from pure surfaces could apply to both CO deposition on and CO desorption from the surfaces of ice mixtures.

Analysis of the pre-exponential factors in terms of activation entropies has revealed that for the water and methanol surfaces, we can consider desorption to proceed *via* a loose transition state. A similar interpretation is also likely for the NH_3 surface but there we must recognize that the entropy of the adsorbed CO may well be significantly higher than on the water and methanol surfaces due to the smaller E_{des} and more effective diffusion of CO over the NH_3 ice surface.

ACKNOWLEDGEMENTS

The authors acknowledge the support of the UK Science and Technology Facilities Council (STFC, ST/M001075/1), the UK Engineering and Physical Science Research Council (EPSRC, EP/D506158/1), and the European Community FP7-ITN Marie-Curie Programme (LASSIE project, grant agreement no. 238258). ST thanks STFC for a project studentship.

DATA AVAILABILITY

The data underlying this article will be shared on reasonable request to the corresponding author.

REFERENCES

Allouche A., Verlaque P., Pourcin J., 1998, J. Phys. Chem. B, 102, 89
Attard G., Barnes C., 1998, Surfaces, Oxford University Press, Oxford
Campbell C.T, Sellers J.R.V., 2012, J. Am. Chem. Soc., 134, 18109
Collings M.P., Dever J.W., Fraser H.J., McCoustra M.R.S., Williams D.A., 2003a, ApJ, 583, 1058
Collings M.P., Dever J.W., Fraser H.J., McCoustra M.R.S., 2003b, Astrophys. Space Sci., 285, 633
Collings M.P., Frankland V.L., Lasne J., Marchione D., Rosu-Finsen A., McCoustra M.R.S., 2015, MNRAS, 449, 1826
Doronin M., Bertin M., Michaut X., Phillipe L., Fillion J.–H., 2015, J. Chem. Phys., 143, 084703
Fayolle E.C., Balfe J., Loomis R., Bergner J., Graninger D., Rajappan M., Öberg K.I., 2016, ApJ, 816, L28
Fraser H.J., Collings M.P., McCoustra M.R.S., 2002, Rev. Sci. Instrum., 73, 2161
Hasegawa T.I., Herbst E., Leung C.M., 1992, ApJS, 82, 167
He J., Acharyya K., Vidali G., 2016, ApJ, 825, 89
Hessey S.G., Jones R.G., 2015, Surf. Int. Anal., 47, 587

King D.A., 1975, Surf. Sci., 47, 384
Noble J.A., Congiu E., Dulieu F., Fraser H.J., 2012, MNRAS, 421, 768
Nørskov J.K., Studt F., Abild-Pedersen F., Bligaard T., 2014, Fundamental Concepts in Heterogeneous Catalysis, Wiley, Hoboken, New Jersey, USA
Penteado E.M., Walsh C., Cuppen H.M., 2017, ApJ, 844, 71
Redhead P.A., 1962, Vacuum, 12, 203
Smith R.S., May R.A., Kay B.D., 2016, J. Phys. Chem. C, 120, 1979
Tait S.L., Dohnalek Z., Campbell C.T., Kay B.D., 2005a, J. Chem. Phys., 122, 164707
Tait S.L., Dohnalek Z., Campbell C.T., Kay B.D., 2005b, J. Chem. Phys., 122, 164708
Tait S.L., Dohnalek Z., Campbell C.T., Kay B.D., 2005c, J. Chem. Phys., 125, 234308
Taj S., 2019, Laboratory Astrochemistry of Dust and Ice, PhD thesis, Heriot-Watt University, Edinburgh, UK
Taj S., Baird D., Rosu-Finsen A., McCoustra M.R.S., 2017, Phys. Chem. Chem. Phys., 19, 7990
Taj S., Baird D., Rosu-Finsen A., McCoustra M.R.S., 2019, Phys. Chem. Chem. Phys., 21, 21633
Thrower J.D., 2009, Laboratory Investigations of the Thermal and Non-thermal Desorption of Aromatic Hydrocarbons in the Interstellar Medium, PhD thesis, Heriot-Watt University, Edinburgh, UK
Thrower J.D., Collings M.P., Rutten F.J.M., McCoustra M.R.S., 2009a, MNRAS, 394, 1510
Thrower J.D., Collings M.P., Rutten F.J.M., McCoustra M.R.S., 2009b, J. Chem. Phys., 131, 244711
Woodruff D.P., Delchar T.A., 1994, Modern Techniques in Surface Science, 2nd edn, Cambridge University Press, Cambridge

SUPPORTING INFORMATION

Supplementary data are available at *MNRAS* online.

MNRAS - CO TPD Paper - ESI - Final - Revised - Accepted.docx

Please note: Oxford University Press is not responsible for the content or functionality of any supporting materials supplied by the authors. Any queries (other than missing material) should be directed to the corresponding author for the article.

This paper has been typeset from a Microsoft Word file prepared by the author.